

Mass divergences in two-particle inelastic scattering

Stephen B. Libby and George Sterman*

Institute for Theoretical Physics, State University of New York at Stony Brook, Stony Brook, New York 11794
(Received 17 August 1978)

Feynman integrals for two-particle inelastic scattering are studied in the limit that the ratio of particle masses to all relevant invariants vanishes. The discussion applies to renormalizable field theories including quantum chromodynamics. Dominant contributions arise from momentum configurations which recall the parton model. The results can be applied to cross sections for single-particle or multiparticle inclusive reactions and to cross sections averaged over small regions of phase space.

I. INTRODUCTION

One of the main challenges of strong-interaction physics is to reproduce the successes of the parton model¹ from quantum chromodynamics² (QCD). The characteristic feature of applications of the parton model is the use of the impulse approximation. That is, scattering processes involving high-mass final states are described by the incoherent sum of *single hard scatterings* of individual components of the original hadron(s).

Thus the leptoproduction total or jet cross section at high Q^2 is assumed to be governed by the point scattering of a single charged parton, while the hadron-hadron production of high-mass pairs of muons or wide-angle hadronic jets is assumed to be dominated by the pointlike interaction of two partons, one from each hadron.¹

In a quantum field theory, the parton-model *Ansätze* and their systematic higher-order corrections can be derived if two requirements are met: (1) The theory should have a small effective coupling³ $\bar{g}(Q^2)$ at high Q^2 so that the Feynman diagrams with the fewest vertices can dominate the cross section if Q^2 is large enough, and (2) there should be no mass divergences such as $\log(Q^2/m^2)$ in the quantities for which we hope to make a perturbative prediction. Such logarithms invalidate the perturbation expansion by making it a power series in $\bar{g}(Q^2) \log(Q^2/m^2)$. They also indicate the importance of long distance effects, for which perturbation theory may be unreliable.

QCD satisfies the first requirement because it is asymptotically free,³ but the second requirement depends on the process considered. In general, some kind of phase-space averaging over jetlike configurations in the final state is necessary to obtain a totally mass-independent cross section, such as in e^+e^- annihilation.^{4,5} Failing that, it may be possible to factorize a cross section or functional thereof into perturbative (mass independent) and "nonperturbative" (mass dependent "wave function") parts.

For the *total* leptoproduction cross section, as is well known, the Wilson operator-product ex-

pansion⁶ guarantees such a factorization for appropriate moments of the cross section.

Mueller proposed⁷ an extension of this type of factorization to other inelastic processes. In particular, he found such a factorization of moments of one-particle inclusive annihilation in ϕ^4 theory and proposed that it might also be proved in QCD perturbation theory. Politzer extended this conjecture to massive- μ -pair production in hadron-hadron scattering,⁸ and recent work has confirmed it.^{9,10}

In this paper, we prove to all orders in perturbation theory for any renormalizable field theory including QCD, that for two-body scattering processes giving rise to any highly inelastic final state, the cross sections are dominated by a single hard scattering.

If there were no mass dependence at all in the cross section, the process could be thought of as a completely short-distance phenomenon. We will show, by a direct examination of Feynman integrals, that short-distance interactions with large momentum transfers take place at a single point. This is the key to a QCD formulation of the intuitive parton picture and its systematic higher-order corrections in light of points (1) and (2).

Our result is applicable to jet and massive-lepton-pair production in lepton-hadron and hadron-hadron scattering as well as to single-particle or multiparticle inclusive cross sections in e^+e^- annihilation. We have used it elsewhere¹⁰ to prove factorization in jet and lepton-pair production in lepton-hadron scattering and (subject to certain assumptions) in hadron-hadron scattering.

Our proof is based on power counting in a totally massless field theory. Although in this application we are looking for the class of graphs that give mass divergence, the techniques we use can also give an upper bound for the power behavior of nondivergent graphs.

II. ZERO-MASS LIMIT FOR TWO-PARTICLE INELASTIC SCATTERING

In this section we describe our approach to mass divergences in perturbation diagrams. We

are interested in final states with particles produced at wide angles relative to the initial directions. If we study single or multiparticle inclusive cross sections, certain line energies may be fixed. Otherwise, we always deal with cross sections integrated over a small region in final-state phase space. We study asymptotic properties and therefore neglect nonleading contributions suppressed to order m^2/E^2 where m is any fixed mass scale and E is the initial center-of-momentum energy. In perturbative calculations the remaining mass dependence turns out to be logarithmic and is therefore associated with divergence in the limits $E \rightarrow \infty$ and $m \rightarrow 0$.

To identify interesting mass dependence we study the limit $m \rightarrow 0$ in the relevant Feynman diagrams. This limit is chosen for convenience and in general should only be considered as a "bookkeeping" device. Only for quantities which turn out to be finite in the zero-mass limit is any real connection with a truly zero-mass theory proposed. We do not even claim that such a theory exists, only that certain quantities can be calculated "as if" it did. Physical masses are taken to zero, while the renormalization mass is taken to be of the same order as the energy.

The discussion in this paper is quite general, and applies to any theory without super-renormalizable interactions whose vectors are Abelian or non-Abelian gauge particles. The diagrams discussed in the text will be drawn without distinguishing particle type. Here, as in Refs. 5 and 10, it turns out to be useful to work in a noncovariant gauge in which longitudinal polarization does not propagate for vector lines. This may be an axial gauge¹¹ (whose propagators introduce additional singularities in Feynman integrals which, however, decouple from cross sections), or one of the class of noncovariant complex gauges of Ref. 5. We need not make the choice explicit at this point.

A general perturbative contribution to a $2 \rightarrow n$ process may be represented as in Fig. 1, where $\Gamma_L^{(\alpha)}$ and $\Gamma_R^{(\alpha)}$ are the vertex function diagrams formed by cutting graph Γ . Such a contribution will be referred to generically as $T_\Gamma^{(\alpha)}$.

The external lines of Γ may be either elementary or composite particles. We can introduce special vertices in the perturbation diagram to represent wave functions where external composite particles couple to any number of internal elementary lines. Our only assumption about the wave functions is a standard one: that they fall off more rapidly than perturbation theory as any of the "constituent" elementary lines increases its invariant mass or transverse momentum relative to the composite particle direction. This means

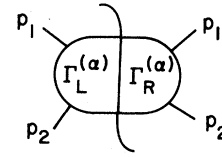


FIG. 1. Cut-graph contribution to a $2 \rightarrow n$ cross section.

that any region in the loop momentum space where one or more constituent lines has invariant mass of order E^2 is automatically suppressed by a power of E^2 relative to what would have been found with only elementary vertices.

The normalization of the wave function requires that it be defined with an overall factor which may be inversely proportional to some power of a fixed mass. Aside from such factors, the presence of wave functions can only *suppress* the behavior of the Feynman integral in the zero-mass limit, and therefore the discussion will be carried out entirely in terms of elementary external lines. We re-emphasize that none of the details of the wave function are necessary to these arguments—all we have assumed is that a cutoff in constituent momenta exists.

We now come to the central observation on which the entire remaining discussion is based: Mass divergences in $T_\Gamma^{(\alpha)}$ come from "pinch singular points"¹² in n -particle phase space and $\Gamma_{L(R)}^{(\alpha)}$ loop momentum space where uncut lines go on-shell in such a way that integrals are *trapped* at the corresponding singularity. Otherwise, the integrals defining $T^{(\alpha)}$ can be evaluated after a deformation of contours chosen to avoid the singular point altogether.

The singular points at which integrals are trapped are characterized by a simple condition: The reduced diagram formed by contracting all lines off-shell at the singular point must represent a physically realizable process in space-time.¹³ This means that each vertex in the reduced diagram may be taken to represent a space-time point, connected by the free propagation of the lines. If all lines are massless, this propagation is always on the light cone. Lines carrying zero momentum have infinite wavelength and can connect any two vertices in this picture. Figures 2(a) and 2(b) give simple examples illustrating these principles. Both are possible reduced diagrams for some $\Gamma_L^{(\alpha)}$ with vectors indicating the direction of spatial momenta for each line in some frame. In our diagrams, the S_i denote soft vertices (where, at the singular point, threshold rearrangements of parallel momenta take place) and

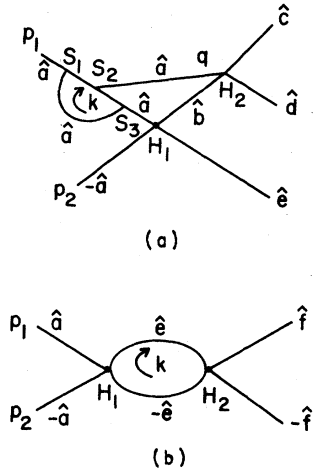


FIG. 2. (a). Example of reduced diagram of graph at pinch singular point. The H_i and S_j denote hard and soft vertices, respectively. The lower case letters $\hat{a}, \hat{b}, \hat{c}$, etc. denote the directions of jet-related lines. (b). An example of a nonpinch reduced diagram.

the H_i denote hard vertices (where scatterings occur above threshold).

The k loop momentum in the graph of Fig. 2(a) is trapped at its singular point, while the one in Fig. 2(b) is not. This is because the lines emitted at vertex S_1 can both arrive at the space-time point corresponding to S_3 , since they both travel at the same velocity (the speed of light) in the same direction. The emission of a line at S_2 makes no difference. In Fig. 2(b), on the other hand, there is no way in which two lines emitted at vertex H_1 and traveling in opposite directions can arrive at vertex H_2 after free propagation. The existence of pinch singular points is a useful condition for mass divergence, but it is only a necessary condition, and can be strengthened.

In Ref. 5 a power-counting prescription has been developed to determine whether or not the integral in the neighborhood of a given pinch singular point can give rise to a mass divergence in partially integrated cross sections.

The advantage of this point of view is that it affords a systematic way of studying the behavior of an arbitrary Feynman integral. Our procedure consists of starting with the most general class of pinch singular points and then using power counting to show that most of them do not lead to mass divergences. By this we do not necessarily mean that the integral over the neighborhood of a pinch singular point is finite. In loop momentum space, pinch singular points lie on multidimensional surfaces. Power counting is done in terms of the "normal" variables which parametrize the space locally perpendicular to each surface. The remaining variables which parametrize the surface

itself, are called "intrinsic", by way of contrast. The precise nonzero energy of any particular line is always an intrinsic variable. Fixing one or more such energy, as in multiparticle inclusive cross sections, therefore does not affect our reasoning.

The more lines that go on-shell at a given pinch singular point, the lower the dimension of the surface. For example, suppose

$$l_1^2 = l_2^2 = \dots = l_N^2 = 0$$

on a surface S_1 of pinch singular points. There will in general be at least one other surface S_2 of pinch singular points, containing S_1 , where

$$l_1^2 = l_2^2 = \dots = l_M^2 = 0, \quad M < N.$$

It may happen that power counting indicates that points on S_1 do not give divergence. This simply means that integrating over some region ζ where l_1 through l_N are constrained to go on-shell together, leads to a finite result. For example, ζ may be defined so that for all $1 \leq i, j \leq N$,

$$\epsilon < \left| \frac{l_i^2/E_i}{l_j^2/E_j} \right| < \frac{1}{\epsilon}, \quad (2.1)$$

with ϵ some fixed small number. Obviously, the intersection of ζ with S_2 consists entirely of S_1 . Notice that some of the normal variables of S_1 are intrinsic variables of S_2 . Power counting must be performed again for S_2 , and it may well indicate the possibility of divergence. If S_2 leads to divergence and S_1 does not, it simply means that, as the intrinsic variables of S_2 are integrated over, no additional logarithms develop when they pass through the subsurface S_1 .

These observations suggest the spirit in which we mean our reduced diagrams to be interpreted. Lines which are contracted in a reduced diagram are not necessarily off-shell everywhere in the range of the integral being discussed. We only require that when they are pinched on-shell within the integration range, it is at singularity surfaces which do not give rise to logarithmic enhancements.

We also stress at this point that the power-counting scheme we apply to our study of cut graphs appropriate to inelastic final states can be applied to any graph where we choose to force some set of lines to be at a singular point (such as in an amplitude as distinct from a cross section), even if in fact it is possible to deform the contours of integration away (a nonpinch surface).

The reduced diagram of any singular point can be decomposed into two subgraphs, one consisting of all lines with zero momentum, the "soft sub-diagram", the other of all lines with finite momentum. The finite-momentum subgraph can itself

be split into “jet subgraphs”, each made up of a set of lines (possibly only one) with precisely parallel spatial momenta. Each such jet subgraph has a set of internal loop momenta and a set of independent finite external momenta. These will be referred to as “jet momenta” below. Among them are p_1 and p_2 which will be called “external graph momenta.” A nontrivial example of a jet subgraph is given by the lines labeled by \hat{a} in Fig. 2a. The internal loop k of the graph is also an internal loop for the \hat{a} jet, and p_1 and q may be taken as its independent jet momenta. Roughly speaking, one can associate the soft subdiagram with “infrared” divergences, and the jet subgraphs with “collinear” divergences.

We now give four necessary conditions at a general pinch singular point for maximal divergence. Maximal divergence will turn out to be logarithmic. The power counting leading to these conditions is the same as in Ref. 5.

- (A) The external lines of the soft subdiagram are vector lines only.
- (B) The external lines of the soft subdiagram attach to jet subdiagrams at three-point vertices only.
- (C) Within each jet subdiagram, no vertices connect more than four lines.
- (D) Any jet is connected to any hard vertex by at most one line.

Condition (D) plays an important role in proofs of factorization.¹⁰ It holds only in the noncovariant gauges where longitudinal polarizations do not propagate on vector lines. To see how it comes about, consider a vertex connecting three vectors of momentum l , l' , and $-l-l'$. The vertex is associated with a sum of numerator momentum factors, each of which contracts with a gluon propagator. Consider a pinch singular point where all three lines are in a jet, so that their momenta are proportional. In the axial gauge,¹¹

$$k_\mu \Delta_{\mu\nu}(k) = \frac{1}{k \cdot n} \left(-n_\nu + \frac{k_\nu}{k \cdot n} \right), \quad (2.2)$$

and one of the line denominators is cancelled at any such pinch singular point. (It is easy to verify that integrating over the subspace $k \cdot n = 0$ leads to no enhancement. See Appendix A of Ref. 10). Numerator momentum factors perpendicular to the jet direction are unsuppressed, but they vanish at least as fast as the square root of l^2 or l'^2 near the singular point.

Now consider a pinch singular point whose reduced diagram has no soft lines, and jets with only two external momenta. Each jet then forms a self-energy, as in Fig. 3(a). In this case, dimensional analysis indicates logarithmic divergence for the internal integrals of each jet subdiagram.

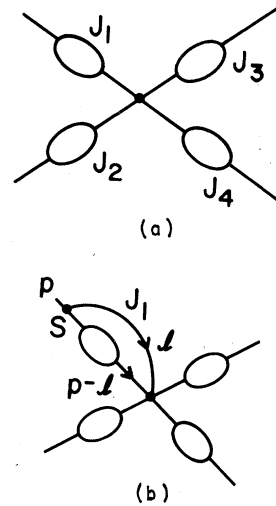


FIG. 3. (a). An example of a reduced diagram with only jet “self-energies” that has logarithmic divergence. (b). Same reduced diagram with additional jet external momentum attached to hard vertex. This case is power suppressed in the axial gauge.

Next, consider Fig. 3(b), where a single line has been added to J_1 . All the jets are still self-energies, except for J_1 , which now has an extra external momentum attached at three-point vertex S . The power counting for all the other jets is still logarithmic, but in J_1 there are now two new internal lines, l and $p-l$, and two conditions on the new loop momentum l , $l^2 = l \cdot p = 0$. In the Feynman gauge, where longitudinal polarization can propagate, there is no suppression from the three-point vertex, and the power counting remains logarithmic. In the axial gauge, however, this possibility is eliminated by (2.2). This reasoning is easily generalized to arbitrary order.

In other gauges longitudinal polarizations can propagate, so point (D) no longer holds. The final result, that only graphs with one hard vertex can give divergence, is gauge invariant. Without point (D), however, the two-particle reducibility of the final reduced-diagram pinch singular points discussed in Ref. 10 would not hold and thus the implementation of the final convolution form for the processes considered in Ref. 10 would be more difficult.

III. ANALYSIS OF HARD INTERACTIONS

In the last section we pointed out that momentum-space configurations which give rise to mass divergences must correspond to physically realizable processes in space-time. These processes involve the scattering of “jets”, consisting of lines with finite energy, and soft lines. We also pointed out that, in the axial gauge, the integral

is suppressed for any momentum configuration where more than one line from any jet subdiagram attaches to a hard vertex. In the space-time picture, this means that only one particle from each jet is involved in each of the hard-scattering "events". This is suggestive of a parton picture of hard scattering. In this section, we deepen this correspondence by showing that the interaction producing large transverse momentum occurs at a single point in space-time. That is, we apply power counting to prove the following statement.

Proposition. Divergence at any pinch singular point is never worse than logarithmic. Pinch singular points of $T_F^{(\alpha)}$ which give logarithmic divergence as $m/E \rightarrow 0$ have only one hard vertex on either side of cut α . Pinch singular points whose reduced diagrams have two or more hard vertices can be integrated over without producing any enhancements in the integral.

Before giving the proof, we observe that the result is strongly suggested by the space-time picture of $2 \rightarrow n$ scattering. Consider, for example, Fig. 2(a). Hard vertices H_1 and H_2 are both connected to the vertex S_2 by lightlike paths, parallel to \hat{a} , while they connect to each other by another lightlike vector \hat{b} . H_1 and H_2 must be at the same point in space-time. It would not be surprising if this restriction in configuration space were associated with a suppression in momentum space, and this turns out to be the case.

This example generalizes to all orders. All particles of jets which include one of the external lines (referred to below as "forward jets") are at the same point in space at any given time. This is because they are all connected by parallel lightlike paths to the same first interaction in the jet, where the single external line "decays" into several parallel-moving particles. But then, all lines in the two jets intersect at the same point P . A hard interaction at P may produce new jets, but since the products of the scattering are all moving away from P at the speed of light, further interaction can take place only between parallel-moving lines. There are therefore no new hard interactions. Zero-momentum (infinite wavelength) lines can always be exchanged between jets, but this, of course, involves no new hard vertices. This picture is special to the case of two particles in the initial state. It does not generalize to three or more.

We now go on to prove the proposition. As we will see, the power-counting result applies to a large class of singular points, including all pinch singular points.

It should be commented here that the power-counting methods we develop in this paper apply to give an upper bound to all pinch singular points

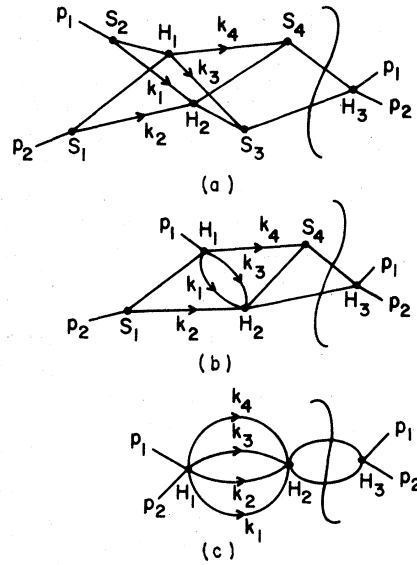


FIG. 4. (a). Reduced diagram representing a contribution to an elastic scattering cross section, in this case, the interference of a single hard scattering and a Landshoff diagram (Ref. 14). Here it is illustrated as an "ordered" singular point. (b). Same diagram after jet reduction of lines k_1 and k_3 and soft vertices S_2 and S_3 . (c). Same diagram after total jet reduction.

in two-body hard scattering, including those which are not divergent. An example of such an application is to the Landshoff-type elastic scattering graphs¹⁴ [such as Fig. 4(a)] where our power-counting bound is actually saturated.

Lemma 1. The power-counting degree of divergence for a singular point (pinch or not) with K connected jet subdiagrams in its reduced diagram is bounded from below by

$$P = D - \sum_{i=1}^K \frac{1}{2}(n_i - 1) - K + 4. \quad (3.1)$$

Here n_i is the number of independent external momenta of the i th jet, including external graph momenta. Consider the set of normal variables whose vanishing ensures that all finite external jet momenta go on-shell in the specified directions, for fixed external graph momenta p_1 and p_2 . Normal variables are chosen so that denominators in each jet depend on them linearly near the singular point. The volume of the region in loop momentum space where the absolute value of every normal variable is bounded by a small number λ is λ^D . In the space of normal variables, λ^D is the scaling behavior of the volume element times the Jacobian of transformation from loop momenta to normal variables.

Proof. Equation (3.1) is proved by a straightforward reapplication of the power counting of Ref. 5.

Without going into the details, some light may be shed on this rather unintuitive formula by the example of Figs. 2 and 3. As described in the last section, adding an extra independent line to any jet leads to, at most, two new dominators if the attachment is made at a three-point vertex. The momentum factors associated with the vertex lead to a numerator suppression of the order of the square root of the denominator size near the singular point. This is the source of the factor $\frac{1}{2}$ in (3.1). P positive in (3.1) indicates no divergence, and $P=0$ logarithmic divergence. Equation (3.1) holds in general only for the noncovariant gauges mentioned above, where longitudinal momentum does not propagate. In particular, it is derived using condition (D) of the last section: That jet subdiagrams are connected to hard vertices by only one line. Other cases are easily seen to be suppressed by a power relative to (3.1). This means, for example, that there is no hard vertex with forward scattering.

Definition. An "ordered" singular point is one at which vertices may be ordered so that energy always flows to the right in the corresponding reduced diagram, which will also be referred to as ordered. This is equivalent to the condition that in no loop of the reduced diagram does energy flow in the same sense as the loop momentum for every line in the loop. Ordering is a necessary, but not sufficient, condition for a singular point to be a pinch singular point.

The proposition is to be verified by finding a lower bound on D in (3.1). D depends only on how jet momenta scatter at hard vertices; it is independent of the internal structure of the jet subdiagrams. To make it easier to study, we construct a method for the further simplification of reduced diagrams to a form which exhibits only the relevant structure. Here and in the rest of the proof, soft lines are neglected. Their presence does not affect the arguments given below.

Lemma 2. The reduced diagram R of any ordered singular point may be further reduced by the contraction of lines to another ordered "jet-reduced" diagram \hat{R} with only hard vertices, connecting lines from more than one jet subdiagram. The total number of vertices in \hat{R} is the number of hard vertices in R , and the number of lines in \hat{R} is

$$N_{\hat{R}} = \sum_{i=1}^K n_i - 4. \quad (3.2)$$

Proof. If R has any soft vertices at all, there is at least one subset of lines l in R , which directly connects a "soft" vertex s to a hard vertex v . If there is more than one s , pick the one closest in ordering to v . Similarly, if there are several

v 's, pick the one closest in ordering to s . Assume s is before v . Contracting the lines l to a point reduces the number of soft vertices by one, leaves the number of hard vertices the same, and preserves the ordering of the remaining vertices and lines so long as there is no vertex t such that energy flows from s to t and from t to v . Is there, then, always at least one pair of vertices s and v which satisfy this condition? They can be found as follows. If such a t exists, there is an alternate path of energy flow from s to v passing through t . By construction, the first vertex in this path after s cannot be hard, and the last vertex before v cannot be soft. Therefore, along the path there is at least one pair of hard and soft vertices such that the soft vertex is to the left of the hard vertex and is connected to it by at least one line. We call this pair s' and v' . Now either the line (s) l connecting s' and v' can be contracted while preserving the order of other lines, or not. If not, the construction may be repeated to find a third pair s'' and v'' . Eventually, the original condition must be satisfied, since there are only a finite number of vertices in the graph. This gives a procedure for contracting lines which can be continued until all soft vertices are eliminated. Finally, if in the diagram which results from eliminating all soft vertices, two hard vertices are connected by two or more parallel lines, these lines are replaced by a single line which carries their total momentum. Then the number of lines left in each jet subdiagram is just the number of independent finite external momenta of the jets, less the number of external lines of the graph. As an example of the reduction process, consider Fig. 4 which includes a Landshoff diagram.¹⁴ Figure (4c) is the final jet-reduced form.

Lemma 3. Suppose \hat{R} is a jet-reduced diagram of T_T with more than one vertex. The entire external momentum of \hat{R} flows through a single initial and single final vertex (\hat{R} therefore looks like a vacuum polarization graph.)

Proof. By the construction of Lemma 2, and because there are only two incoming and outgoing lines, all soft vertices to the left of the first hard vertex H_1 are contracted into H_1 , while all those to the right of the last one H_V are contracted into H_V . But then all momentum flows through H_1 and H_V . Notice that this result, on which the following discussion depends, is specific to two-particle scattering.

Lemma 4. $P=0$, and there is logarithmic divergence only if

$$n_i = 1, \quad i = 1, \dots, K. \quad (3.3)$$

Otherwise, $P > 0$.

Proof. Consider an arbitrary ordered jet-re-

duced diagram \hat{R} . As observed in the proof of Lemma 2, any line momentum $k_\alpha^{(i)}$ of \hat{R} may be considered as the α th finite jet momentum of jet subdiagram i . At the singular point, all the $k_\alpha^{(i)}$ of jet i must be lightlike and parallel, while the precise direction of the jet may or may not be constrained. These conditions, which are not necessarily independent, are satisfied when the following variables vanish:

$$(k_\alpha^{(i)})^2, \text{ all } i \text{ and } \alpha, \tag{3.4}$$

$$\frac{k_\alpha^{(i)} \cdot k_1^{(i)}}{(k_\alpha^{(i)})_0 (k_1^{(i)})_0} = 1 - \cos \theta_\alpha^{(i)} \sim \frac{1}{2} (\theta_\alpha^{(i)})^2.$$

The $\theta_\alpha^{(i)}$ measure the angles between each momentum $k_\alpha^{(i)}$ in jet i , and a "reference" momentum $k_1^{(i)}$ for that jet chosen arbitrarily. The four external momenta p_1 and p_2 fix the direction of the forward jets, and they are always chosen as reference momenta. The momenta in the i th jet depend linearly on the variables (3.4).

We can now go on to estimate the volume in loop momentum space where each of the variables in (3.4) is bounded in absolute value by a small parameter λ ,

$$|(k_\alpha^{(i)})^2| < \lambda, \frac{1}{2} (\theta_\alpha^{(i)})^2 < \lambda. \tag{3.5}$$

First we note that the $(k_\alpha^{(i)})^2$ are obviously all independent, so that the volume associated with their subspace is λ^p , where $p = \sum_{i=1}^K n_i - 4$. The more difficult question is how to bound the volume associated with the angular variables. It is at this point that the jet-reduced diagram becomes useful. It enables us to find an upper bound on the volume for each choice of reference and nonreference momenta.

Suppose H_1 and H_2 are the first two vertices in jet-reduced diagram \hat{R} . Because \hat{R} is ordered, and all momentum must flow through H_1, H_2 must be connected to H_1 by a set I_{12} of ζ_{12} lines, $\zeta_{12} \geq 2$, all from different jets, forming $\zeta_{12} - 1$ loops. An example with $\zeta_{12} = 4$ is Fig. 4(c). Setting the lines of I_{12} on shell, we can find the volume in phase space where (3.5) is satisfied.

Let f_{12} be the number of lines in I_{12} which are nonreference. It is convenient to treat each of the following four cases separately:

- (1) $f_{12} = \zeta_{12}$,
- (2) $1 < f_{12} < \zeta_{12}$,
- (3) $f_{12} = 1$,
- (4) $f_{12} = 0$.

(1) Here we can start by choosing the first $\zeta_{12} - 1$ of the line momenta $l_j^{(12)}$ connecting H_1 with H_2 as independent loop momenta. The $\theta_\alpha^{(i)}$ for each of

these lines can then be chosen as the polar angle for each loop. The corresponding volume is $\lambda^{\zeta_{12}-1}$. This leaves the cosine of the angle $\theta_\beta^{(k)}$ of the last line. There are three possibilities:

(a) The spatial momenta $\vec{l}_j^{(12)}, j < \zeta_{12}$, span the three-dimensional space. Then $\cos \theta_\beta^{(k)}$ is independent of the preceding angles, and the corresponding volume is $\lambda^{\zeta_{12}}$.

(b) The spatial momenta $\vec{l}_j^{(12)}, j < \zeta_{12}$ are restricted to a plane at the singular point. In this case $\vec{l}_{\zeta_{12}}^{(12)}$ is automatically in the same plane at the singular point and the volume element is of order $\lambda^{\zeta_{12}-1/2}$.

(c) The $\vec{l}_j^{(12)}, j < \zeta_{12}$ are restricted to a line. Then $\vec{l}_{\zeta_{12}}^{(12)}$ is automatically restricted to the same line, and there is no further suppression of the volume element, which remains of order $\lambda^{\zeta_{12}-1}$.

(2) The same reasoning as in (1) gives a maximum volume element of $\lambda^{\zeta_{12}-1+\nu}$ with $\nu = 1, \frac{1}{2}$, or 0, in cases (a), (b), and (c), respectively.

(3) In this case, the volume element is always at most λ . When the reference momenta span three-dimensional space, $\cos \theta_\beta^{(k)}$ of the nonreference momentum is an independent variable, even if the reference momenta are chosen as loop momenta. On the other hand, if the reference momenta do not span the space, the nonreference momentum may be chosen as a loop momentum. Such a choice does not lead to an underestimate of the volume, since by assumption not all the reference momenta are independent at this point.

(4) The volume is independent of λ in this case.

Suppose we now contract the ζ_{12} lines which make up I_{12} . Because all momenta arriving at H_2 must come from H_1 , the result is another ordered jet-reduced diagram \hat{R}' , with another set of lines I'_{12} connecting its first two vertices. The volume element from the loop momenta of this subdiagram can be estimated by just the same rules as above, independently of I_{12} . This procedure can be continued until, after $V-1$ steps, with V the number of vertices in \hat{R} , the full diagram \hat{R} has been reduced to a single vertex.

The volume element found in this way is bounded from above by λ^{D_0} , where

$$D_0 \geq \left(\sum_{i=1}^K n_i - 4 \right) + \frac{1}{2} \sum_{i=1}^K (n_i - 1). \tag{3.6}$$

The first term comes from the $(k_\alpha^{(i)})^2$, and the second from the phase-space volume found above.

If there are any non-reference momenta at all, the power of λ in the phase-space volume for any set of lines I_{12} is always greater than or equal to $\frac{1}{2} f_{12}$, and is an equality only when $f_{12} = \zeta_{12} = 2$. The choice of reference momenta within a jet can be made to get the best bound possible. In the absence of forward scattering at any hard vertex, it

is always possible to choose reference momenta so that not all nonreference momenta are paired in this way. Then (3.6) is an equality only when (3.3) holds, that is, when there are no nonreference momenta at all.

Substituting (3.6) into (3.1) gives

$$P \geq 0, \tag{3.7}$$

where again, (3.7) is an equality only when (3.1) is satisfied. Divergence is therefore at worst logarithmic.

Lemma 4 enables us to prove the proposition easily. Because of Lemma 4, forward jets attach to only one hard vertex on either side of the cut. But then, all momentum not in the forward jets must be emitted from hard vertex V on the left, and absorbed at hard vertex V' on the right, as in Fig. 5, where soft lines have been reintroduced in the subdiagram G_s . The subgraph H in Fig. 5 has the same momentum-space structure as a cut vacuum polarization diagram. It will be referred to below as the "hard subdiagram." Because at a pinch singular point the reduced subdiagram H must represent a physical process on either side of the cut, it cannot contain any hard vertices other than V and V' .

The external jets J_1 and J_2 in Fig. 5 represent jets made up of lines parallel to p_1 and p_2 . These lines play the roles of "spectators" to the hard interaction, and their effects group into a kind of parton distribution function. The analogy to the parton picture is still not complete, however, because zero-momentum lines have not yet been dealt with. They can connect to either jet and to the hard subdiagram. The hard scattering is therefore not yet independent of the spectator particles, nor are the spectators of each external jet

independent of each other.

The question of how to deal with zero-momentum lines is taken up in Ref. 10 where the complete factorization of lepton-hadron production of inelastic jets and/or lepton pairs is proved in QCD. For hadron-hadron scattering, we prove complete factorization for totally massless QED. In the latter theory the interaction of truly soft spectators (G_s in Fig. 5) are nontrivial as in QCD since multiphoton scattering can be divergent when the fermions are massless. These divergences can be eliminated by a sum over the emission of soft particles. We believe that such a proof can be carried out for QCD as well.

The argument of Ref. 10 proceeds by summing over the cuts of subdiagram H depicted in Fig. 5, and then summing over soft emissions due to cuts of G_s . Then, we found that the remaining mass divergence of the cross section takes on a simple form of the convolution of a mass-independent hard scattering subprocess $M(k^2, \dots)$ (which depends on the nonforward invariant mass k^2) with the "spectator" processes that make up the forward jets J_i . For leptonproduction, the result is

$$\sigma(p_1, p_h, k) = \text{disc} \int_{k^2/s}^1 dx M_i(k, p_i, xp_h) J_{th}(xp_h, p_h), \tag{3.8}$$

where p_i and p_h are, respectively, the incident lepton and hadron momenta. For hadron-hadron scattering it is

$$\begin{aligned} \sigma(p_1, p_2, k) = \text{disc} \int_0^1 dx_1 dx_2 \theta(x_1 x_2 s - k^2) \\ \times (J_1)_{h_1 t_1}(x_1 p_1, p_1) \\ \times M_{t_1 t_2}(x_1 p_1, x_2 p_2, k) \\ \times (J_2)_{t_2 h_2}(x_2 p_2, p_2), \end{aligned} \tag{3.9}$$

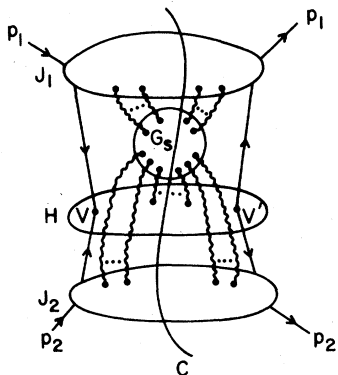


FIG. 5. General reduced diagram giving remaining mass divergence for a $2 \rightarrow n$ inelastic process. J_1 and J_2 are the two forward jets. The blob H containing a single hard vertex V on either side of the cut is the hard-scattering subdiagram. The blob G_s represents the truly infrared divergences that couple the forward jets and the hard subdiagram.

where p_1 and p_2 are the incident hadron momenta. In Eqs. (3.8) and (3.9), gauge dependence has been suppressed. Following Mueller⁷ and Politzer⁸ one may then factorize these convolutions by taking appropriate moments. The factored mass divergence, associated only with the forward jets, is given by the matrix elements of the same twist-two operators¹⁵ as for the total leptonproduction cross section. Likewise, deviations from parton-like scaling of the hard-scattering part M_{it} , are given by the anomalous dimensions of these operators.

Thus the high-energy approximation to such jet cross sections does not involve particularly detailed properties of the hadron wave functions. In parton language, all that appears is the amplitude that a hadron of momentum P have a given parton with momentum fraction xP . The analogous final quantities in these cross sections in the field theory formalism are the forward matrix elements of

the relevant operators. By way of contrast, the result *does not* depend on the amplitude that a pair of partons have, respectively, momentum fractions xP and yP of the original hadron momentum P . Such details of the wave function could be important for processes with more than one hard vertex. As Landshoff has pointed out,¹⁴ this may

be the case in wide-angle elastic scattering of bound states.

ACKNOWLEDGMENT

This work was supported in part by the National Science Foundation under Grant No. PHY-76-15328.

*Address, after September 1, 1978: Institute for Advanced Study, Princeton, New Jersey 08540.

¹R. P. Feynman, *Photon-Hadron Interactions* (Benjamin, New York, 1972); D. J. Gross, in *Methods in Field Theory*, 1975 Les Houches Lectures, edited by R. Balian and J. Zinn-Justin (North-Holland, Amsterdam, 1976); J. Ellis, in *Weak and Electromagnetic Interactions at High Energy*, 1976 Les Houches Lectures, edited by R. Balian and C. H. Llewellyn Smith (North-Holland, Amsterdam, 1977).

²H. Fritzsch, M. Gell-Mann, and H. Leutwyler, *Phys. Lett.* **47B**, 365 (1973); D. J. Gross and F. Wilczek, *Phys. Rev. D* **8**, 3633 (1973); S. Weinberg, *Phys. Rev. Lett.* **31**, 494 (1973).

³D. J. Gross and F. Wilczek, *Phys. Rev. Lett.* **30**, 1343 (1973); H. D. Politzer, *ibid.* **30**, 1346 (1973); G. 't Hooft (unpublished).

⁴G. Sterman and S. Weinberg, *Phys. Rev. Lett.* **39**, 1436 (1977); H. Georgi and M. Machacek, *ibid.* **39**, 1237 (1977); E. Farhi, *ibid.* **39**, 1587 (1977); S. S. Shei, New York University Report No. NYU/TR 14/77, 1977 (unpublished); A. Raychaudhuri, Oxford Report No. 19/78, 1978 (unpublished).

⁵G. Sterman, *Phys. Rev. D* **17**, 2773 (1978); **17**, 2789 (1978).

⁶K. Wilson, *Phys. Rev.* **179**, 1499 (1969).

⁷A. Mueller, *Phys. Rev. D* **9**, 963 (1974).

⁸H. D. Politzer, *Phys. Lett.* **70B**, 430 (1977); *Nucl. Phys.* **B129**, 301 (1977).

⁹R. Ellis, H. Georgi, M. Machacek, H. Politzer, and G. Ross, *Phys. Lett.* **78B**, 281 (1978); A. Mueller, *Phys. Rev. D* **18**, 3705 (1978).

¹⁰S. Libby and G. Sterman, *Phys. Lett.* **78B**, 618 (1978); *Phys. Rev. D* **18**, 3252 (1978).

¹¹R. I. Arnowitt and S. I. Fickler, *Phys. Rev.* **127**, 1321 (1962); W. Konetschny and W. Kummer, *Nucl. Phys.* **B100**, 106 (1975); H. Kluberg-Stern and J. B. Zuber, *Phys. Rev. D* **12**, 482 (1975); **12**, 3159 (1975); J. Frenkel, *ibid.* **13**, 2335 (1976); A.

Sugamoto, H. Yamamoto, and N. Nakagawa, Univ. of Tokyo Report No. UT-291, 1977 (unpublished).

¹²R. J. Eden, P. V. Landshoff, D. I. Olive, and J. C. Polkinghorne, *The Analytic S-Matrix* (Cambridge Univ. Press, New York, 1966); G. Sterman, Ref. 5.

¹³S. Coleman and R. E. Norton, *Nuovo Cimento* **38**, 438 (1965).

¹⁴P. V. Landshoff, *Phys. Rev. D* **10**, 1024 (1974).

¹⁵D. J. Gross and S. B. Treiman, *Phys. Rev. D* **4**, 1059 (1971).